

Lasers in Manufacturing Conference 2019

## Increasing heat transfer of metals through periodical microstructures using Direct Laser Interference Patterning

Sabri Alamri<sup>a\*</sup>, Frederic Schell<sup>a</sup>, Tobias Steege<sup>a</sup>, Andrés F. Lasagni<sup>a,b</sup>, Tim Kunze<sup>a</sup>

<sup>a</sup>Fraunhofer-Institut für Werkstoff- und Strahltechnik IWS, Winterbergstraße 28, Dresden 01277, Germany

<sup>b</sup>Technische Universität Dresden, Institut für Fertigungstechnik George-Bähr-Str. 3c, Dresden 01069, Germany

---

### Abstract

The increasing number of micro-electronic components per unit area led not only to an increase of computing power but also to an increase of the device's operating temperature. Heat sinks, equipped with macroscopic fins or pins, dissipate heat by increasing the surface area. In this work, a microscopic approach for improving the heat transfer of metals is presented, aiming to increase the surface area by fabricating periodical microstructures. Direct Laser Interference Patterning has been used for fabricating microstructures on stainless-steel plates employing a nanosecond IR laser. A statistical design of experiment was used for optimizing the structuring parameters and maximizing the surface area. The heat dissipation properties, evaluated with a heat flux sensor, were correlated with the developed surface area, finding a clear trend. In particular, the microstructuring permitted to increase the surface area up to 280%, which lead to an increase of heat transfer by 23.8%.

Keywords: Heat Transfer; microstructures; DLIP;

---

### 1. Introduction

In the last years, the impressive developments in the field of micro-technology led to the production of electronic devices, whose components got significantly faster and smaller. This led also to an enormous increase of the processing power. Nevertheless, together with the smaller size of the semiconductor devices also the operating temperature increases. A higher temperature implies a lower conductivity of the doped semiconductors devices and thus lower performances, as reported by Pecht, 1998. Therefore, cooling strategies have become crucial in order to guarantee an optimal device operation.

---

\* Corresponding author. Tel.: +49-351-83391-3007; fax: +49-83391-3300 .  
E-mail address: sabri.alamri@iws.fraunhofer.de .

Cooling is usually performed with macroscopic heat sinks built from materials having high heat conduction properties. Typical heat sink designs use an array of fins or pins to maximize the surface of the heat sink, which leads to a higher heat transfer to the surrounding medium, as investigated by Lee, 1995. Nevertheless, this approach encounters difficulties when the elements to be cooled are integrated components and of the size of a few millimeters or even less. The choice of the heat sink material plays also an important role for guaranteeing a high heat transfer. In fact, among metals, copper and aluminum alloys are usually employed for the fabrication of heat sinks, as stated by Geffroy, 2008.

As commonly known, an increase of the surface area improves the heat exchange property of metals, which is at the base of the heat sink principle. An interesting point is to investigate whether the ability of a surface to dissipate heat also improves in the microscopic scale, by using micro- or nano-structured heat-conducting materials.

In the work of Ayer, 2011 the role of the surface roughness of aluminium surfaces on the heat transfer was investigated. As a result, a higher roughness increases the amount of transferred heat, which is in agreement with the general rule of the increase in the surface area. Moreover, in the work of Jones, 2009 the change in the pool boiling of surfaces with different roughness and contact angles has been systematically investigated, finding that for roughness values greater than  $1\text{ }\mu\text{m}$  the heat transfer coefficient increases significantly. On the other hand, Ventola, 2014 investigated the heat properties of laser sintered heat sinks, finding that for roughened surfaces the heat transfer increases up to a peak value of 73%, in comparison to flat surfaces. Additionally, surface roughness also affects the emissivity of a body, consequently influencing the radiative heat transfer. As demonstrated by Vorobyev, 2009, the production of microstructures on the filament of a tungsten lamp a significant increase of the emissivity was observed.

Among the mask-free, contactless and single-step microfabrication methods, laser micromachining achieved a dominant position in several industry-oriented fields. A well-established laser technique able to produce periodical structures in the micro- and sub-micrometer range is Direct Laser Interference Patterning (DLIP). This method relies on the overlap of two or more coherent laser beams on the sample, where an interference pattern is created. At the maxima positions the material is directly treated, while at the minima it remains unaffected. For a given laser wavelength and number of beams, the pattern period can be easily adjusted by modifying the angle, the polarization and the intensity of the interfering beams, as described by Voisiat, 2011. Recently, this technique was successfully used to pattern a wide range of materials such as metals, ceramics and polymers with processing speeds reaching  $1\text{ m}^2/\text{min}$ , as shown by Lang, 2016.

In this work line-like microstructures are fabricated on stainless steel plates through DLIP with different spatial periods and depths. The heat transfer characteristics of these surfaces are then systematically investigated, aiming to find a correlation between the topographical parameters and the heat transfer. A statistical approach (Design of Experiment, DoE) has been implemented for choosing the structuring parameters with the aim to maximize the heat transfer. Confocal microscopy as well as scanning electron microscopy have been used in order to assess the morphological and topographical aspect of the textured surfaces, respectively.

## 2. Materials and Methods

A two-beam interference setup was utilized to produce line-like surface patterns (Fig. 1a). The employed laser is an IR (1053 nm) Q-switched diode pumped solid state laser (Laser Export, TECH-1053 Basic) with a pulse duration of 15 ns, a repetition rate of 1kHz and a maximal pulse energy of 500  $\mu\text{J}$ . The experiments were conducted on a compact self-developed DLIP system (DLIP- $\mu\text{FAB}$ , Fraunhofer IWS) producing pixels containing the line-like interference pattern with an estimated diameter of 90  $\mu\text{m}$ . To cover larger areas, the

substrate was translated in x and y directions and a specific distance between the pixels is defined. The pulse-to-pulse distance in the direction parallel to the interference lines (X-direction) defines the pulse overlap, while the pixel separation in the direction perpendicular to the interference pattern (Y-direction) defines the hatch distance (Fig. 1b). The optical DLIP module is designed to split the main beam into two beams using a diffractive optical element, which are later recombined using a prism and a lens. By varying the distance between the prism and the lens, the spatial period of the lines can be adjusted by the user between  $1.45\ \mu\text{m}$  and  $8.5\ \mu\text{m}$ . For each experiment, the laser fluence has been retrieved measuring the laser power distribution and estimating the area in which the two laser beams interfere.

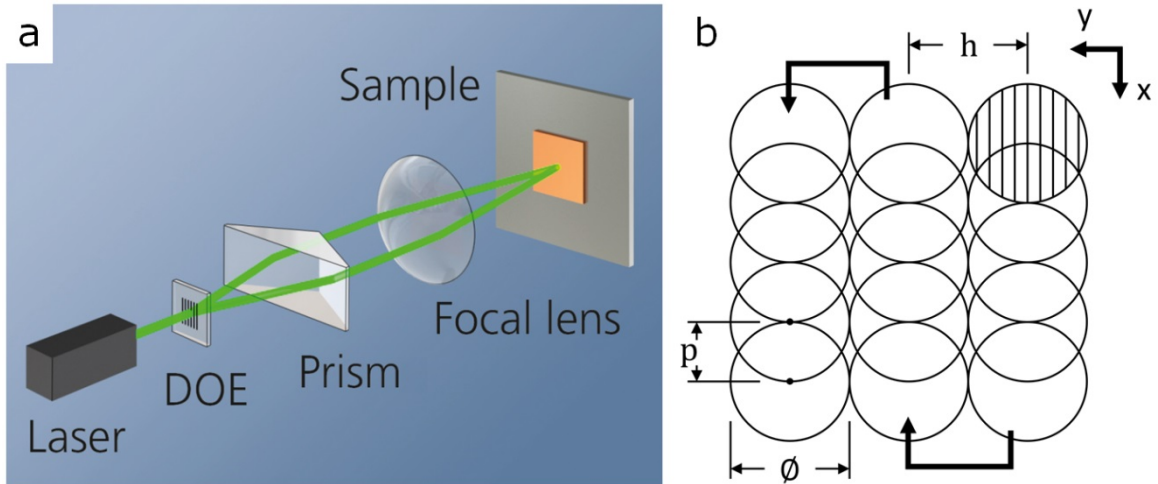


Fig. 1. (a) Schematic of the DLIP setup; (b) representation of the structuring approach.

The dependency of the developed surface area on the laser parameters is investigated following a DoE plan that varies three different parameters (factors). The plan is based on a two-level factorial design which tests each factor at two specific values (levels), forming a cube in a three-dimensional factor space where each corner point of the cube represents on combination of factors at specific levels. In order to account for non-linear behavior of the developed surface area, this design is extended by a center point in the middle of the cube and six star points that extend beyond the surface of the cube.

The morphology of structured samples was characterized using confocal microscopy (Leica DCM 3D) employing a 50x magnification objective with a nominal lateral resolution of 340 nm and vertical resolution of 4 nm. The structures are evaluated in terms of surface area increase compared to an unstructured surface. In particular the developed surface area value (Sdr) has been taken into account, which describes the ratio of the real surface area to the projected surface area. In order to obtain the real surface area from a measured sample, the software *Gwyddion* has been used. Topographical inspections have been carried out also by means of Scanning Electron Microscopy (JEOL JSM 6610LV) without any previous surface treatment.

Although copper and aluminium are a common choice for heat sinks due to their high thermal conductivity, in this work stainless steel plates have been chosen due to their superior processability employing infrared and nanosecond laser radiation, in comparison with copper or aluminium. The austenitic stainless steel X5CrNi18-101 with a thermal conductivity of 15 W/mK is used to carry out the experiments. Flat samples with dimensions of  $15 \times 15\ \text{mm}^2$  and a thickness of 1 mm have been used for the laser structuring and subsequent measurement of the heat flux.

In order to measure the change in the heat transfer, a self-designed setup has been built, as depicted in Fig. 2. The heat flux sensor (greenTEG, gSKIN-XP-26-9C) is mounted onto a heating resistor and the sample on top of the sensor by using thermal compound. A PT-1000 temperature sensor is in contact with the heating resistor, at the bottom of the setup. Cork plates are used to isolate the whole setup in every direction except the direction of heat flux (vertical direction). The heating resistor is controlled by a control circuit built with an Arduino microcontroller, which keeps the temperature at a constant value of 80 °C as measured by the temperature sensor. The heat flux sensor is connected to a data logger (National Instruments, USB-6009), from which the voltage signals are retrieved using the software LabView SignalExpress 2012. The signals are recorder after 20 minutes in order to guarantee the steady state condition, while the data are recorded for 30 minutes, in order to average any environmental fluctuation. The measurements are conducted in a temperature controlled lab at a constant ambient temperature of 22°C in order to guarantee a constant temperature gradient between the heating resistor and the ambient air.

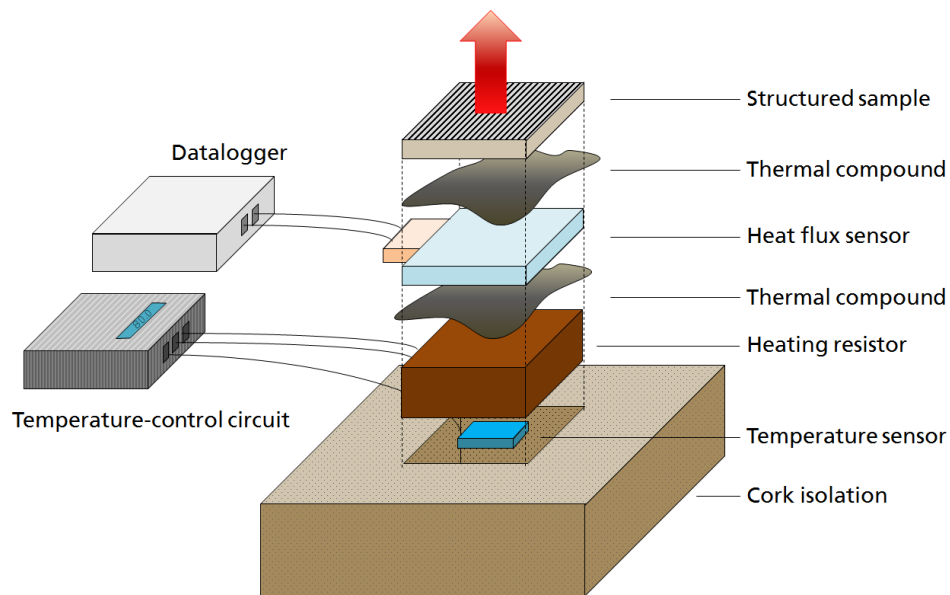


Fig. 2. Representation of the heat flux measuring system.

### 3. Results and Discussion

For the structuring experiments a Central Composite Design (CCD) DoE was used considering the laser fluence, the pulse-overlap (which can be expressed in pulses per pixel area,  $P/px$ ) and the spatial period as factors while the hatch distance has been kept constant at a value of 30  $\mu m$ , adjusted to the closest integer multiple of the spatial period to avoid inhomogeneities. The DoE has been designed in order to maximize the developed surface area values, which are retrieved by confocal measurements and elaborated by the model. After a reduction of the parameters giving negligible contributions to the DoE, the retrieved model represents the experimental data with a coefficient of determination ( $R^2$ ) of 86.1%.

Using the generated regression function, the model's response can be visualized as a contour plot, as depicted in the example of Fig. 3a, keeping the period constant to a value of  $7.7\ \mu\text{m}$ . As it can be seen from the diagram, the value of the Sdr increases with increasing laser fluence and pulse overlap values, reaching values of around 360 % (that is 3.6 times the surface of an unstructured sample). In order to measure the change in the heat transfer properties, six sets of parameters yielding increasing Sdr values have been selected from the model (red dots in Fig. 3a) for the central overlap value of 80 P/px, which gives the highest prediction accuracy of the model. Therefore six stainless steel samples have been textured varying the laser fluence from  $0.85\ \text{J}/\text{cm}^2$  to  $1.60\ \text{J}/\text{cm}^2$  and keeping the spatial period constant at  $7.7\ \mu\text{m}$ , the pulse overlap at 80 P/px and using a hatch distance of  $30.8\ \mu\text{m}$ .

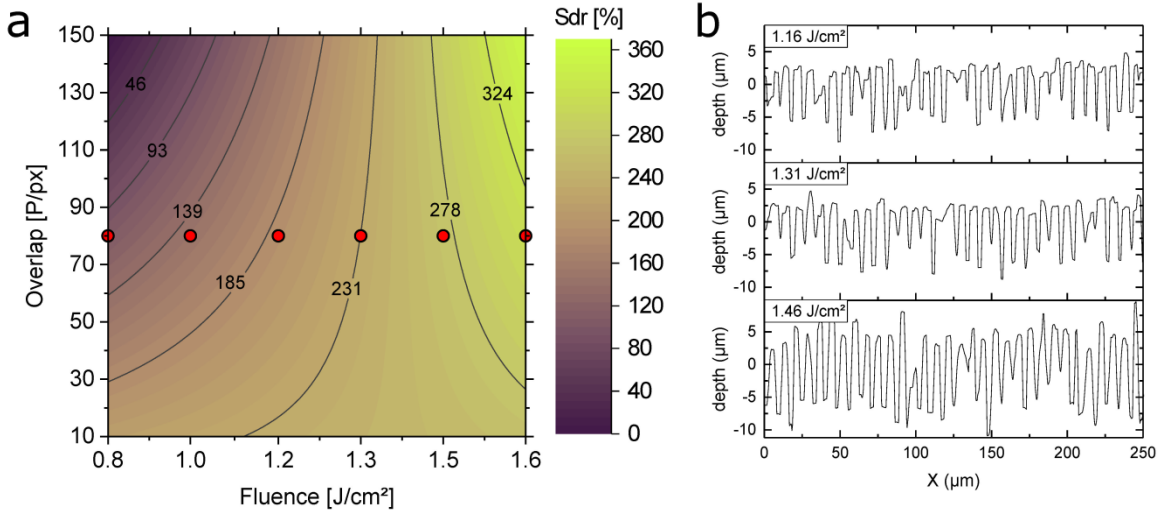


Fig. 3. (a) Retrieved model for the variation of the Sdr as a function of the employed laser fluence and pulse overlap; (b) confocal structure profiles for three different laser fluences and a pulse overlap of 80 P/px.

Examples of the generated surfaces are represented in the confocal profiles of Fig. 3b, showing the change in the surface morphology for increasing laser fluence. As it can be noticed, a structure height greater than  $10\ \mu\text{m}$  could be reached employing a laser fluence of  $1.46\ \text{J}/\text{cm}^2$ . Moreover, thanks to the accurate distribution of the interference pixels for at the given hatch distance (equals to four times the spatial period), the overall appearance of the sample results in a high texture homogeneity. This can be noticed in the SEM image in Fig. 4a, for an area much larger than the interference area itself. As commonly known for nanosecond laser processing, the texturing is driven by thermal ablation processes, leading to the formation of a melting front, which highly contributes to the formation of the microstructures. Fig. 4b depicts a high magnification topography of the microstructures, giving an impression of the formation process of the micro-lines. As it can be noticed from Fig. 4b, the crest of the lines (corresponding to the interference minima) appears irregular and porous, where the voids can be ascribed to the sealing of two melting fronts coming from two adjacent interference maxima, as explained by Lang, 2019.

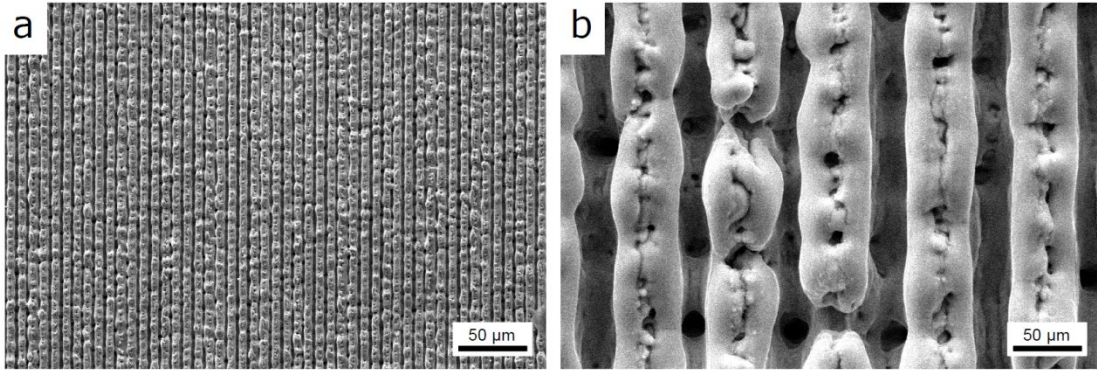


Fig. 4. (a) top-view SEM image of the sample textured with a laser fluence of  $1.46 \text{ J/cm}^2$  and a pulse overlap of 80P/px ; (b) high-magnification of Fig.4a

In Figure 5a, the developed surface area of the six samples and the prediction interval of the model are plotted as a function of the fluence used for the manufacturing process. As it can be noticed, a Sdr value of nearly 280 % can be reached for a laser fluence of  $1.46 \text{ J/cm}^2$ . Nevertheless, although the Sdr directly increases for increasing laser fluence values, a discrepancy between the measured values and the ones predicted by the regression model can be found. In particular, for the central fluence values the Sdr values follow precisely the predictions, while for low or high fluence values the accordance lowers. Since the full range of fluence used in the DoE-experiment was used to produce these samples, this discrepancy in the peripheral area may be caused by the decreasing predictive capabilities of the model near the edge of the parameter space.

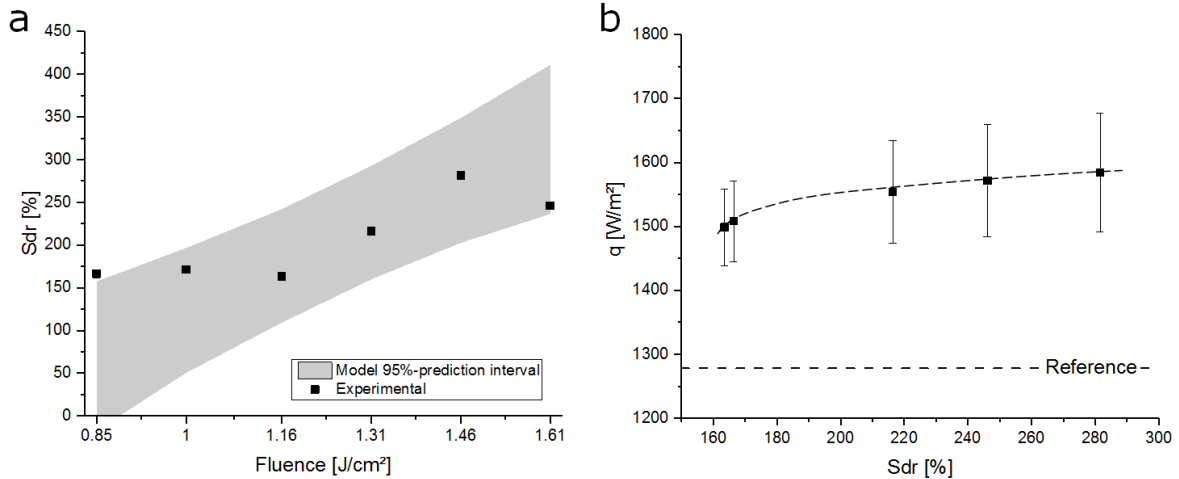


Fig. 5. (a) Trend of the Sdr as a function of the laser fluence for a pulse overlap of 80 P/px including the model's prediction (grey) and the Sdr measurements for the replicated samples; (b) change in the heat flux as a function of the developed surface area.

Afterwards, the heat flux density of each sample was measured and a direct comparison with the developed surface area is reported. The reference unstructured plate (Sdr = 1) shows a heat flux density of  $1279.6 \text{ W/m}^2$ , while the laser-treated samples always exhibit higher heat flux density values. The heat flux

measurements relative to the chosen fluence values have been plotted as a function of the produced surface area in Fig. 5b, showing a direct correlation between the increase of the developed surface area and the heat flux. In particular for a Sdr value of 280% the heat flux measured through the stainless steel plates increases by nearly 24%.

Although the heat flux density increases with the developed surface area, the trend is not linear and a saturation for high Sdr values is visible. This behavior can be attributed to several factors. Firstly, while extending the surface area of a plane surface yields a homogeneous increase of the heat flux density, a surface area increase by means of a roughness enhancement creates micro-valleys and -heights having different temperatures and heat transfer characteristics. Moreover, further alterations on the surface after the laser treatment are likely to modify the thermal characteristics of the material. For instance, chemical changes on the surface of metals (mostly oxidation) create a layer which may show different thermal properties with respect to the bulk material. On the other hand, the presence of porosity in the microstructures (as shown in Fig. 4b) allows the embedding of air, which lowers the heat transfer coefficient of the stainless steel.

#### 4. Conclusions

In this work Direct Laser Interference Patterning has been used in order to fabricate periodic line-like microstructures on stainless steel plates, aiming to change the heat transfer characteristics of the material. The influence of the laser parameters such as laser fluence, pulse overlap, hatch distance and spatial period, on the developed surface area of the samples have been characterized with the help of a statistical design of experiments. After identifying the key parameters which produce a remarkable increase in the developed surface area, a set of samples with a targeted surface area increase have been selected and tested on a self-developed heat transfer measuring platform.

The relationship between the heat flux density change and the developed surface area follows a positive trend and therefore confirms the initial assumption, that an increase of surface area in the microscopic regime causes an increase of heat flux. However, other surface parameters are changed with the laser processing, such as geometrical and chemical factors, which affect the heat transfer of the metal plates, possibly reducing the effectiveness of the increase of the surface area. In order to exclude one or the other factor, further experiments employing different wavelength, pulse duration and shape of the microstructures are envisaged.

#### Acknowledgements

The work of S.A. was supported by the Laser4Fun project ([www.laser4fun.eu](http://www.laser4fun.eu)), funded from the European Union's Horizon 2020 research and innovation programme under the Marie Skłodowska-Curie grant agreement No. 675063. The work of A. L. is also supported by the German Research Foundation (DFG) under Excellence Initiative program by the German federal and state governments to promote top-level research at German universities.

#### References

- Pecht, M., Lall, P. & Hakim, E. B., 1998. The influence of temperature on integrated circuit failure mechanisms in High-Temperature Electronics
- Lee, S. 1995. Optimum Design and Selection of Heat Sinks. IEEE Trans. Components Packag. Manuf. Technol. Part A.

- Geffroy, P. M., Mathias, J. D. & Silvain, J. F. 2008. Heat sink material selection in electronic devices by computational approach. *Adv. Eng. Mater.*
- Ayer, M. R. A 2011. Study of the Influence of Surface Roughness on Heat Transfer.
- Jones, B. J., McHale, J. P. & Garimella, S. V. 2009. The Influence of Surface Roughness on Nucleate Pool Boiling Heat Transfer. *J. Heat Transfer*
- Ventola, L. et al. 2014. Rough surfaces with enhanced heat transfer for electronics cooling by direct metal laser sintering. *Int. J. Heat Mass Transf.*
- Vorobyev, A. Y., Makin, V. S. & Guo, C. 2009. Brighter light sources from black metal: Significant increase in emission efficiency of incandescent light sources. *Phys. Rev. Lett.*
- Voisiat, B., Gedvilas, M., Indrišinas, S. & Račiukaitis, G. 2011. Picosecond-laser 4-beam-interference ablation as a flexible tool for thin film microstructuring. *Phys. Procedia* 12, 116–124.
- Lang, V., Roch, T. & Lasagni, A. F. 2016. High-Speed Surface Structuring of Polycarbonate Using Direct Laser Interference Patterning: Toward  $1 \text{ m}^2 \text{ min}^{-1}$  Fabrication Speed Barrier. *Adv. Eng. Mater.* 18, 1342–1348.
- Lang, V., Voisiat, B., Kunze, T. & Lasagni, A. F. 2019. Fabrication of High Aspect-Ratio Surface Micro Patterns on Stainless Steel using High-Speed Direct Laser Interference Patterning. *Adv. Eng. Mater.* 0, 1900151.